Resonant longitudinal *Zitterbewegung* in zigzag graphene nanoribbons

S. Ghosh, U. Schwingenschlögl, and A. Manchon*
Physical Science and Engineering Division, King Abdullah University of Science and Technology (KAUST), Thuwal 23955-6900, Saudi Arabia
(Received 21 October 2014; published 8 January 2015)

The *Zitterbewegung* of a wave packet in a zigzag graphene nanoribbon is theoretically investigated. The coupling between edge states and bulk states results in intriguing properties. Apart from the oscillation in position perpendicular to the direction of motion, we also observe an oscillation *along* the direction of propagation which is not present in semiconductor nanowires or infinite graphene sheets. We also observe a resonance of its amplitude with respect to the central momentum of the wave packet. We show here that this longitudinal *Zitterbewegung* is caused by the interplay between bulk and edge states, which is a unique property of a zigzag nanoribbon.

DOI: 10.1103/PhysRevB.91.045409 PACS number(s): 72.80.Vp, 71.70.Ej, 73.63.Nm

I. INTRODUCTION

Zitterbewegung, i.e., the trembling motion of the wave packet, is one of the salient features of a relativistic quantum system that distinguishes it from a nonrelativistic one: the strong locking between the (pseudo)spin degree of freedom and the momentum results in an oscillation of the position of the wave packet as a function of time. Although this effect has drawn significant theoretical attention from the perspective of relativistic theory [1,2] and for the understanding of fundamental physics regarding electron structure [3] and spin [4], its observation has remained an experimental challenge for a long time. Recently, it has been realized that a large class of noncentrosymmetric condensed matter systems [5,6] like nanowires [7–9], two dimensional electron gas [10], and honeycomb lattices [11,12] (e.g., graphene, silicene [13], MoS_2 [14], etc.), surfaces of topological insulators [15,16], photonic crystals [17], and cold atom gases [18–20] can be described by a Dirac-like equation and hence becomes instrumental for the experimental observation of *Zitterbewegung*. All these systems are characterized by a strong coupling between the (pseudo)spin $\hat{\boldsymbol{\sigma}}$ (spin angular momentum, sublattice index, orbital, etc.) and the momentum $\mathbf{k}$, i.e., $\hat{H}_{\rm so} = \xi \hat{\sigma}_i k_j$, which has two main consequences. First, the velocity of the particle depends on the direction of the (pseudo)spin through the so-called anomalous velocity $\partial_{\mathbf{k}} \hat{H}_{\rm so}$. Second, when the particle moves, the (pseudo)spin "feels" an effective magnetic field proportional to the momentum and about which it precesses [5]. *Zitterbewegung* reflects the reciprocal influence of the precessing (pseudo)spin on the anomalous velocity. Hence although the physical details behind the origin of *Zitterbewegung* are different in different noncentrosymmetric systems, they can be described under the framework of a general multiband theory [21].

Among all these systems graphene has captured a large amount of attention in recent years. Among other relativistic phenomena, *Zitterbewegung* [22,23] also has attracted significant theoretical attention for monolayer [24,25] and bilayer [26,27] graphene, carbon nanotubes [28,29], and graphene superlattices [30]. However, in all these cases the *Zitterbewegung* has a transient character [24,30] which makes it hard to observe. This transient behavior is a manifestation of *Riemann-Lebesgue* theorem [2,24], which predicts that if the weight function of the Fourier component is continuous then the wave packet dies off. One way to overcome this damping is to use discretized weight which can be achieved by applying a perpendicular magnetic field [26,31] or pseudomagnetic field induced by strain [32]. The same remedy also works for an asymmetric quantum well [33].

Another way to prevent the damping is to use a transverse confinement. Schliemann *et al.* [7] showed the existence of a *Zitterbewegung* effect for a semiconducting nanowire with a parabolic confinement along the transverse direction. They further show that if the states defined along the direction of motion are degenerate with opposite spin, the *Zitterbewegung* undergoes a resonance.

Motivated by the studies in semiconducting nanowires, we investigate the nature of *Zitterbewegung* for a zigzag graphene nanoribbon (ZGNR). The main characteristic feature that distinguishes a ZGNR from a semiconducting nanowire is the presence of edge states which appear as a result of the coupling between transverse and longitudinal momenta caused by the boundary condition [34,35]. The edge states are distinguished by their low energy which is a result of their strong localization. Although the properties of the edge state have been extensively studied [36,37], the effect of their interaction with the bulk state has not been thoroughly addressed. In this work, we demonstrate that the *Zitterbewegung* effect in ZGNR arises from the overlap between bulk and edge states and enters in resonance when properly weighting the contributions of these two types of states. Even more interestingly the resonance occurs in the direction of propagation, in sharp contrast with other systems (extended graphene, nanowires, etc.).

II. THEORY AND METHOD

The low energy effective Hamiltonian for graphene is given by [12]

$$H_\eta = -i\hbar v_F(\sigma_x \partial_x + \eta \sigma_y \partial_y), \tag{1}$$

where $\eta = \pm 1$ stands for the (K, K') points and v_F is the Fermi velocity. In the following sections we will consider $\hbar = v_F = 1$, for simplicity. For the ZGNR with zigzag edges along the x direction (see Fig. 1), we use the boundary

*aurelien.manchon@kaust.edu.sa

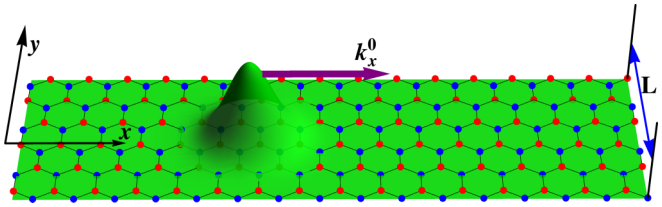

FIG. 1. (Color online) Schematic of the initial wave packet at time $t = 0$ in a zigzag graphene nanoribbon.

condition $\phi_A^K(y = L) = \phi_A^{K'}(y = L) = \phi_B^K(y = 0) = \phi_B^{K'}(y = 0) = 0$ [12], L being the width of the ribbon and the suffix A, B denoting the type of sublattice. For ZGNR, the solutions around K and K' points are decoupled and we can proceed with any one of them separately (see Fig. 3). In the following, we will consider only the K ($\eta = 1$) point. The wave function is given by

$$\psi_s(k_n,k_x,x,y) = A_n \begin{pmatrix} s\ \sin(k_n(y-L)) \\ \sin(k_n y) \end{pmatrix} e^{ik_x x},$$
$$A_n = \left(L - \frac{\sin(2k_n L)}{2k_n}\right)^{-\frac{1}{2}}, \tag{2}$$

where $s = \pm 1$ for positive/negative energy states. k_n corresponds to the nth mode of transverse momentum k_y which is related to k_x by the relation

$$k_x = \frac{k_n}{\tan(k_n L)}, \tag{3}$$

and the corresponding energy eigenvalue is given by

$$E^s = s\left|\frac{k_n}{\sin(k_n L)}\right|. \tag{4}$$

A detailed derivation of these expressions can be found in Sec. H.1. in Ref. [12]. In the present work, once k_x is fixed, k_n are calculated numerically. The solutions of Eq. (3) are reported on Fig. 2. Note that, for $k_x L > 1$, there exists an imaginary root for k_n that represents the edge states (red dashed line in Fig. 2).

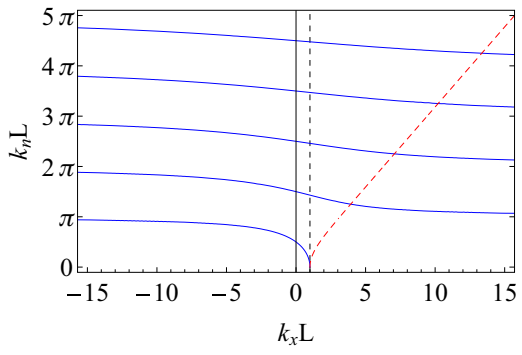

FIG. 2. (Color online) Variation of k_n with k_x near $K(k_x = 0)$ point. The solid blue and the red dashed lines are respectively the real and imaginary solution for k_n and correspond to the bulk and the edge states. The imaginary solution (edge state) appears for $k_x L \geqslant 1$, the limiting value ($k_x L = 1$) being denoted by the vertical black dashed line.

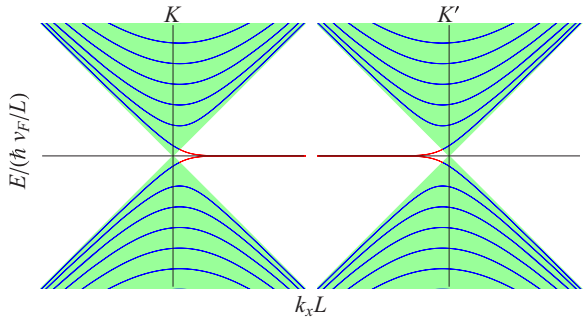

FIG. 3. (Color online) Band structure of a ZGNR near the K and K' points. The blue lines are due to the bulk state and the red lines are due to the edge states. The green region denotes the continuous spectrum for an infinite graphene sheet.

The band structure calculated from Eq. (4) is displayed in Fig. 3. The two K and K' valleys are clearly separated and possess both bulk states (blue lines), and edge states (red lines).

The details of the *Zitterbewegung* response are quite sensitive to the specific form of the initial wave packet [29]. In this work we have considered a Gaussian wave packet which is a reasonable assumption to identify the salient features of this effect. For *Zitterbewegung* to take place, the initial wave packet must contain both positive and negative energy components. The wave packet with an initial momentum (k_x^0, k_y^0) reads

$$\Psi(x,y,t) = \frac{1}{\sqrt{2\pi}}\frac{d}{\sqrt{\pi}}\int dk_x \frac{1}{\zeta(k_x)} \sum_{k_n[k_x]} e^{-\frac{1}{2}((k_x-k_x^0)+(k_n-k_y^0))^2 d^2}$$
$$\times \frac{1}{\sqrt{2}}(\psi_+(k_n,k_x,x,y)e^{-iE_n t} + \psi_-(k_n,k_x,x,y)e^{iE_n t}), \tag{5}$$

where $\zeta(k_x) = \sqrt{\frac{d}{\sqrt{\pi}}}\sum_{k_n[k_x]} e^{-(1/2)(k_n-k_y^0)^2 d^2}$. For large ZGNR, the transverse momenta (k_n) will be more closely spaced and $\zeta(k_x) \to 1$. For an infinite graphene sheet k_n is continuous and $\zeta(k_x) = 1$. To any given k_x corresponds a discrete set of k_n which is taken into account by the summation. The expectation values of the position along $\langle x(t)\rangle_\Psi$ and perpendicular $\langle y(t)\rangle_\Psi$ to the direction of motion are defined:

$$\langle x(t)\rangle_\Psi = \int dx\, dy\, \Psi(x,y,t)^\dagger x \Psi(x,y,t), \tag{6}$$

$$\langle y(t)\rangle_\Psi = \int dx\, dy\, \Psi(x,y,t)^\dagger y \Psi(x,y,t). \tag{7}$$

Since the wave packet consists of both positive and negative energy states, the expectation value of an operator also contains two contributions [24]: one nonoscillatory part coming from the individual positive and negative energy states and a second oscillatory part coming from the interference between the positive and negative states which we are interested in. We define the *Zitterbewegung* component of an operator as

$$\mathcal{O}_Z = \langle\mathcal{O}\rangle_\Psi - \tfrac{1}{2}(\langle\mathcal{O}\rangle_+ + \langle\mathcal{O}\rangle_-), \tag{8}$$

where $\langle\mathcal{O}\rangle_{+,-}$ corresponds to the expectation value evaluated for a wave packet made of only positive/negative energy states with the same Gaussian weight as $\Psi(x,y,t)$.

III. RESULT AND DISCUSSION

The zigzag boundary condition not only quantizes k_y but also couples k_x and k_y [see Eq. (3)]. However, in the limit of large k_x, i.e., $|k_x L| \gg 1$, $k_n \to n\pi/L$, which is close to a harmonic oscillator confinement, as seen in Fig. 2. For our analysis we have chosen $k_y^0 = 0$, $-10 \leqslant k_x^0 L \leqslant 14$ as well as different widths d of the Gaussian distribution. The Gaussian width controls the number of transverse modes in the wave packet. The range of k_x^0 covers both the regions where k_ns are almost independent of k_x ($|k_x L - 1| \gg 0$) and where k_ns are strongly dependent on k_x ($k_x L \sim 1$) (Fig. 2). Due to the Gaussian weight, for $k_x^0 L \ll 1$ the wave packet is dominated by bulk states and tends to localize at the center of the ribbon. For $k_x^0 L \gg 1$ the wave packet is dominated by edge states and tends to localize near the edges. Near $k_x^0 L = 1$ both states are present, their relative weight depending on d. These three types of wave packets (bulk dominated, edge dominated, and bulk-edge overlapping) are represented in Fig. 4 at $t = 0$. The overlap between bulk and edge states is the driving factor behind the *Zitterbewegung* in the present system. When both states have comparable share, the resultant wave packet is more delocalized and displays maximum oscillation amplitude.

Let us now investigate the time dependence of the position of the wave packet. Figure 5 shows the expectation values $\langle x(t)\rangle_\Psi$ and $\langle y(t)\rangle_\Psi$ for $k_x^0 = 1/L$ and $d = L/4$. As mentioned above, one can see that the total expectation value is not simply the sum of the individual contributions of positive and negative energy wave packets, but also displays an oscillatory contribution arising from the interplay between these two energy states. Movies of the time evolution of the complete wave packet for different k_x^0 are available in Supplemental Materials [38]. The wave packet consists of both bulk (B) and edge states (E) with both positive (+) and negative energies (−) which produces five types of interference: (i) $B_\pm \leftrightarrow B_\pm$, (ii) $B_\pm \leftrightarrow B_\mp$, (iii) $B_\pm \leftrightarrow E_\pm$, (iv) $B_\pm \leftrightarrow E_\mp$, and (v) $E_\pm \leftrightarrow E_\mp$. Since the edge states have energy close to zero, (v) does not give any significant contribution to oscillation and (iii) and (iv) yield almost similar contributions. The bulk states with the same sign of energy have a smaller gap with respect to that with opposite sign which makes the contribution from (i) also negligible. Hence the dominant contribution will come from (ii) and (iii).

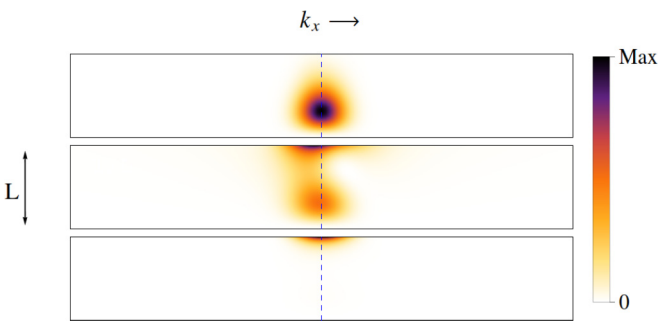

FIG. 4. (Color online) Norm of the wave packet at $t = 0$ for three different values of k_x^0 with $d = L/4$. For $k_x^0 = -8/L$ the bulk states are dominant. For $k_x^0 = 1/L$ both bulk and edge gives the same contribution and for $k_x^0 = 8/L$ the states are localized at the edges. The width of the ribbon is L and the same scale is used for the length. The blue dashed line denotes $x = 0$.

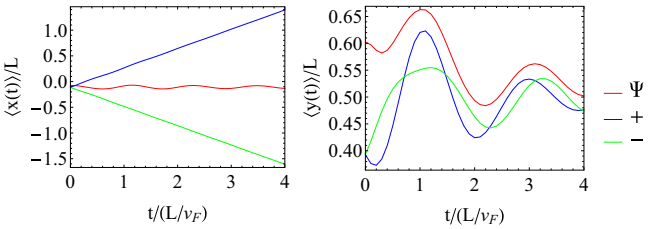

FIG. 5. (Color online) Expectation values for x and y for the complete wave function (Ψ) and for the positive and negative components (+/−), respectively. Here we use $k_x^0 = 1/L$ and $d = L/4$.

Notice that here we considered states at the K valley only. Similar results can be obtained for the K' valley as well, but in that case the values have opposite signs. In principle, intervalley scattering may affect the *Zitterbewegung* effect by enabling destructive interferences between the two valleys. Such intervalley mixing occurs in armchair nanoribbons [12] or in the presence of short-range impurities and defects [39,40], but is absent in defect-free zigzag nanoribbons. Besides, here the width of a momentum space Gaussian wave packet is $\sim 100\ \mathrm{nm}^{-1}$, which is 1000 times smaller than the intervalley separation ($\sim 1\text{Å}^{-1}$) and thus eliminates any possibility of valley mixing so long as we are close to the $K(K')$ point. Still, for a large width or large value of k_x^0, there can be contributions from both valleys that can cancel each other.

Figures 6(a) and 6(b) show $x_Z(t)$ and $y_Z(t)$ for a wave packet with a Gaussian width $d = L/4$. The maximum amplitude

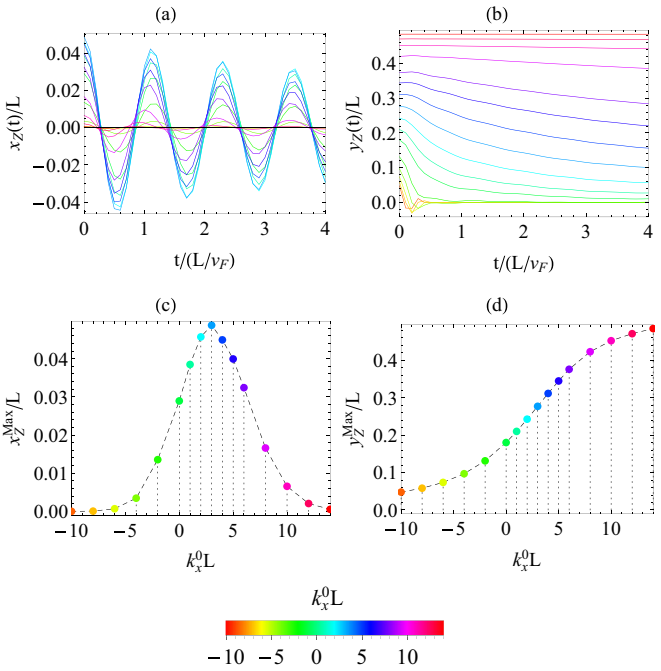

FIG. 6. (Color online) *Zitterbewegung* component of (a) $\langle x(t)\rangle$ and (b) $\langle y(t)\rangle$ for a wave packet with Gaussian width $d = L/4$. (c) and (d) show the variation of amplitude with the central momentum.

$x_Z^{\max}$ and $y_Z^{\max}$ are reported on Figs. 6(c) and 6(d), respectively. One can see that both $x_Z(t)$ and $y_Z(t)$ present a damped oscillatory behavior. In the case of $x_Z(t)$, the decay length is much longer than the oscillation period, while in the case of $y_Z(t)$, the decay is much stronger which suppresses the oscillatory behavior. Note also that the period of oscillation of $x_Z(t)$ is essentially constant $\sim\pi/2$. In addition, $y_Z(t)$ shows a saturation towards $L/2$, which is quite expected as the amplitude cannot exceed the ribbon width. One remarkable difference of the *Zitterbewegung* effect for ZGNR with respect to other Dirac systems is the existence of oscillation *along* the direction of motion, i.e., $x_Z(t)$. If the longitudinal and transverse momenta are not coupled, one can readily check, using a Heisenberg equation of motion, that the oscillation of a Dirac particle is always perpendicular to its initial momentum. However, when the momenta are coupled, a longitudinal component of the oscillation develops causing a longitudinal *Zitterbewegung*.

The other striking characteristic of the *Zitterbewegung* effect is the appearance of a resonance in $x_Z(t)$ oscillations, as shown in Fig. 6(c). From Fig. 2 one can see that the dependence between k_x and k_y is strongly nonlinear near $k_x L = 1$, which corresponds to the rise of edge states. We already showed in Fig. 4 that bulk and edge states tend to localize in opposite ends along the transverse direction. From Fig. 3 one can also see that for a particular k_x the bulk and edge states have opposite propagation velocity as suggested by the slope of the energy bands. Hence maximum oscillation is expected when these two states contribute equally.

This feature can be further clarified when considering different Gaussian widths. Following earlier studies [24] we assume that the envelope of the oscillating $x_Z(t)$ is of an exponential nature, i.e.,

$$x_Z^{\text{envelope}} = x_Z^{\max} e^{-\Gamma t}, \tag{9}$$

where x_Z^{envelope} is the value of $x_Z(t)$ at the peaks which describes the envelope for $x_Z(t)$ and $x_Z^{\max}$ is the maximum peak value. Figures 7(a) and 7(b) show $x_Z^{\max}$ and Γ, respectively, for different values of the width d.

From Fig. 7, one observes that as d decreases (i.e., the wave packet becomes more localized in real space and broader in momentum space), both the amplitude ($x_Z^{\max}$) and damping (Γ) increase. The resonant amplitude however does not increase monotonically and rather tends towards a saturation which is clear from Fig. 7(a). The change of Γ is more prominent when $x_Z^{\max}$ undergoes the resonance. The resonance takes place roughly within the region $2 \lesssim k_x^0 L \lesssim 3$. The larger d, the closer the resonance is to $k_x L = 1$. This behavior can be explained based on our earlier argument. As d increases, less bulk states contribute to the wave packet. Consequently the bulk and edge share a similar amount of contribution and the wave packet becomes more delocalized causing an increase in the amplitude of $x_Z(t)$. Since the contribution from the bulk decreases, the condition when the bulk and edge share equal contribution becomes closer to $k_x L = 1$, and hence the resonant position also shifts accordingly. The damping also depends on the amount of interference among states. For smaller d more states interfere with each other which results in faster damping [see Fig. 7(b)]. It is worth mentioning that the present analysis also holds with

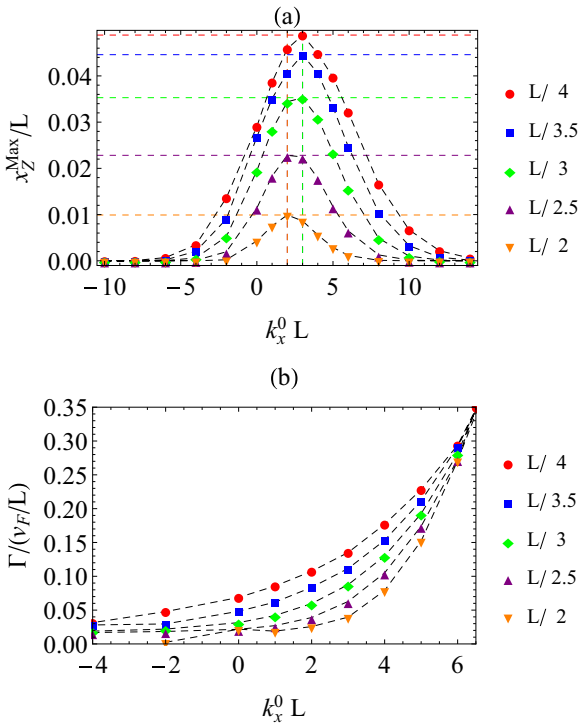

FIG. 7. (Color online) Variation of (a) $x_Z^{\max}$ and (b) Γ with k_x^0 for different d (given in legend).

the current density $j_x = e v_F \langle \sigma_x \rangle$. One can readily see that $v_F \langle \sigma_x \rangle = \langle dx/dt \rangle = \langle dx \rangle / dt$ and hence the qualitative nature of the resonance and damping will be the same.

It is instructive to compare the present results with previous works [7,24,31], which are summarized in Table I. Although the values provided in this table are indicative only, they show that in extended graphene monolayers and bilayers (Gr monolayer and Gr bilayer), the frequency of oscillation is extremely fast ($\tau \sim$ fs) compared to nanoribbons (100 nm ZGNR) and semiconducting nanowires (50 nm InAs) ($\tau \sim$ 0.1–1 ps). Furthermore, the state quantization in extended graphene results in a strong damping of the *Zitterbewegung* effect. This damping can be dramatically reduced by opening Landau levels using a magnetic field (Gr+2.5 T and Gr+10

TABLE I. Comparison between different characteristics of the *Zitterbewegung* in various systems: InAs nanowire, graphene mono and bilayers with and without a magnetic field. The last line presents our results. The quantities represented are the width of the wave packet d, the initial wavelength $\lambda_0 = 2\pi/k_0$, amplitude $x_Z^{\max}$, oscillation period τ, and damping rate Γ^{-1}. In the case of semiconducting nanowire and ZGNR, we use the values at resonance.

System	d (nm)	λ_0 (nm)	$x_Z^{\max}$ (nm)	τ (fs)	Γ^{-1} (fs)
50 nm InAs [7]		95	35	2500	
Gr monolayer [24]	40	5	5	2.5	15
Gr bilayer [24]	30	18	5	2.5	50
Gr+2.5 T [31]	8	18	5	650	900
Gr+10 T [31]	8	10	5	280	350
100 nm ZGNR	25	16	5	100	1000

T), which is accompanied by a slowdown of the oscillation frequency. The results discussed in the present work (100 nm ZGNR) compare favorably with the results obtained using semiconducting nanowires or magnetic field in graphene. It therefore demonstrates that using bulk-edge state overlap to achieve *Zitterbewegung* resonance is a valuable route to observe this effect experimentally.

IV. CONCLUSION

In this work we investigated the *Zitterbewegung* effect in ZGNR and demonstrated that in sharp contrast to other Dirac systems, the trembling motion appears along the direction of propagation of the wave packet. This peculiar feature stems from the coupling between the momenta along longitudinal and transverse direction of motion caused by the zigzag boundary condition. Such a coupling does not exist in armchair nanoribbons. Furthermore, by tuning the initial longitudinal wave vector, the wave packet enters in resonance which results in a significant increase of the magnitude of the oscillation. This resonance is attributed to the interference between the bulk and edge states and appears when these states equally contribute to the wave packet. In fact, the resonant longitudinal *Zitterbewegung* is thus a true signature of the coexistence of bulk and edge states and should be observable in other low dimensional Dirac systems with appropriate edges, such as silicene [41] or MoS_2-like [42] zigzag nanoribbons.

ACKNOWLEDGMENTS

The authors acknowledge fruitful discussions with Professor E. di Fabrizio. Research reported in this publication was supported by the King Abdullah University of Science and Technology (KAUST).

[1] K. Huang, Am. J. Phys. **20**, 479 (1952).
[2] J. A. Lock, Am. J. Phys. **47**, 797 (1979).
[3] A. O. Barut and A. J. Bracken, Phys. Rev. D **23**, 2454 (1981).
[4] A. O. Barut and N. Zanghi, Phys. Rev. Lett. **52**, 2009 (1984).
[5] J. Cserti and G. Dávid, Phys. Rev. B **74**, 172305 (2006).
[6] R. Winkler, U. Zülicke, and J. Bolte, Phys. Rev. B **75**, 205314 (2007).
[7] J. Schliemann, D. Loss, and R. M. Westervelt, Phys. Rev. Lett. **94**, 206801 (2005).
[8] W. Zawadzki, Phys. Rev. B **72**, 085217 (2005).
[9] P. Brusheim and H. Q. Xu, Phys. Rev. B **74**, 205307 (2006).
[10] V. Y. Demikhovskii, G. M. Maksimova, and E. V. Frolova, Phys. Rev. B **78**, 115401 (2008).
[11] A. K. Geim and K. S. Novoselov, Nat. Mater. **6**, 183 (2007).
[12] A. H. Castro Neto, F. Guinea, N. M. R. Peres, K. S. Novoselov, and A. K. Geim, Rev. Mod. Phys. **81**, 109 (2009).
[13] E. Romera, J. Roldán, and F. de los Santos, Phys. Lett. A **378**, 2582 (2014).
[14] A. Singh, T. Biswas, T. K. Ghosh, and A. Agarwal, Eur. Phys. J. B **87**, 275 (2014).
[15] D. Culcer, Phys. Rev. B **84**, 235411 (2011).
[16] D. V. Khomitsky, A. A. Chubanov, and A. A. Konakov, arXiv:1408.1544.
[17] X. Zhang, Phys. Rev. Lett. **100**, 113903 (2008).
[18] J. Y. Vaishnav and C. W. Clark, Phys. Rev. Lett. **100**, 153002 (2008).
[19] R. Gerritsma, G. Kirchmair, F. Zähringer, E. Solano, R. Blatt, and C. F. Roos, Nature (London) **463**, 68 (2010).
[20] L. J. LeBlanc, M. C. Beeler, K. Jiménez-García, A. R. Perry, S. Sugawa, R. A. Williams, and I. B. Spielman, New J. Phys. **15**, 073011 (2013).
[21] G. Dávid and J. Cserti, Phys. Rev. B **81**, 121417 (2010).
[22] M. I. Katsnelson, Eur. Phys. J. B **51**, 157 (2006).
[23] J. Tworzydo, B. Trauzettel, M. Titov, A. Rycerz, and C. W. J. Beenakker, Phys. Rev. Lett. **96**, 246802 (2006).
[24] T. M. Rusin and W. Zawadzki, Phys. Rev. B **76**, 195439 (2007).
[25] G. M. Maksimova, V. Y. Demikhovskii, and E. V. Frolova, Phys. Rev. B **78**, 235321 (2008).
[26] Y.-X. Wang, Z. Yang, and S.-J. Xiong, EPL **89**, 17007 (2010).
[27] E. Jung, D. K. Park, and C.-S. Park, Phys. Rev. B **88**, 039903(E) (2013).
[28] W. Zawadzki, Phys. Rev. B **74**, 205439 (2006).
[29] T. M. Rusin and W. Zawadzki, J. Phys.: Condens. Matter **26**, 215301 (2014).
[30] Q. Wang, R. Shen, L. Sheng, B. G. Wang, and D. Y. Xing, Phys. Rev. A **89**, 022121 (2014).
[31] T. M. Rusin and W. Zawadzki, Phys. Rev. B **78**, 125419 (2008).
[32] A. Chaves, L. Covaci, K. Y. Rakhimov, G. A. Farias, and F. M. Peeters, Phys. Rev. B **82**, 205430 (2010).
[33] T. Biswas and T. K. Ghosh, J. Phys.: Condens. Matter **24**, 185304 (2012).
[34] L. Brey and H. A. Fertig, Phys. Rev. B **73**, 235411 (2006).
[35] K. Wakabayashi, K.-i. Sasaki, T. Nakanishi, and T. Enoki, Sci. Technol. Adv. Mater. **11**, 054504 (2010).
[36] K. Nakada, M. Fujita, G. Dresselhaus, and M. Dresselhaus, Phys. Rev. B **54**, 17954 (1996).
[37] Y.-W. Son, M. L. Cohen, and S. G. Louie, Nature (London) **444**, 347 (2006).
[38] See Supplemental Material at http://link.aps.org/supplemental/10.1103/PhysRevB.91.045409 for a movie displaying the time evolution of a wave packet of width $d = L/4$ for various values of k_x^0, taken between $-10/L$ and $+14/L$.
[39] A. F. Morpurgo and F. Guinea, Phys. Rev. Lett. **97**, 196804 (2006).
[40] J.-H. Chen, W. G. Cullen, C. Jang, M. S. Fuhrer, and E. D. Williams, Phys. Rev. Lett. **102**, 236805 (2009).
[41] M. Ezawa and N. Nagaosa, Phys. Rev. B **88**, 121401 (2013).
[42] E. Erdogan, I. H. Popov, a. N. Enyashin, and G. Seifert, Eur. Phys. J. B **85**, 33 (2012).